J. Biochem. 125, 899-903 (1999)

Crystal Structures of Wild-Type and Mutant Plastocyanins from a Higher Plant, *Silene*[1]

Hajime Sugawara,* Tsuyoshi Inoue,* Chunmin Li,*,[2] Masaharu Gotowda,* Takashi Hibino,† Teruhiro Takabe,† and Yasushi Kai*,[3]

Department of Materials Chemistry, Graduate School of Engineering, Osaka University, Suita, Osaka 565-0871; and †Department of Chemistry, Faculty of Science and Technology, Meijo University, Tenpaku-ku, Nagoya 468-0073

Received November 20, 1998; accepted February 3, 1999

Plastocyanin functions as an electron carrier between the cytochrome b_6f complex and photosystem I. The crystal structures of the wild-type and E43K/D44K double mutant from the higher plant, *Silene*, have been determined at 2.0 and 1.75 Å resolution, respectively. The wild-type plastocyanin comprises two monomers per asymmetric unit, one of which shows the unusually great distance between the copper ion and the $N_{\delta 1}$ atom of H87 because of the hydrogen bond network formation between H87 and symmetry-related G10. The root mean square deviation for Cα atoms between the wild-type and mutant plastocyanins is 0.44 Å, however, the electrostatic potential maps of their molecular surfaces are remarkably different. The low electron-transfer rate in the E43K/D44K mutant results from the hindrance of electrostatic interactions, not from the structural change due to the mutation.

Key words: acidic patch, crystal structure, double mutant, electron transfer, plastocyanin.

Plastocyanin is a blue copper protein which functions as an electron carrier between the cytochrome b_6f complex and $P700^+$ of photosystem I. Plastocyanin is a component of the photosynthetic electron transfer system in higher plants (*1-3*).

A number of three-dimensional structures of plastocyanins have been determined by protein crystallography and NMR methods. In higher plants, the crystal structures of plastocyanins from poplar (*4*) and spinach (*5*), and the solution structures of plastocyanins from French bean (*6*) and parsley (*7*) have been solved. These studies revealed that plastocyanin has a β-sandwich structure composed of eight β-strands. The side chains of H37, H87, C84, and M92 coordinate with the copper atom with a tetrahedral geometry.

Solvent-exposed H87 is located at the hydrophobic site and Y83 at a negatively charged site composed of two acidic patches comprising positions 42 to 45 and 59 to 61. These two sites around H87 and Y83 are considered to be essential for electron-transfer from the results of kinetic studies (*8, 9*). An acidic patch surrounds Y83 and appears to interact with cytochrome *f* and photosystem I (*10*). The residues of both acidic patches in plastocyanin from the higher plant, *Silene* (SilPc), were replaced with asparagine or lysine by site-directed mutagenesis (*11*). Mutants as to residues 59 and 60 do not change the rates of electron-transfer from cytochrome *f* and to $P700^+$ of photosystem I, however, replacement of residues 42-44 decreases both rates. In particular, the E43K/D44K double mutant shows comparative decreases. As a consequence, the acidic patch comprising positions 42 to 45 seems to be important for electron transfer. To determine whether the comparative decrease of the electron-transfer rate in the case of the mutant SilPc is due to the structural difference or to the difference in the electrostatic potential map on the molecular surface between the wild-type and mutant SilPcs, we have solved the crystal structures of both the wild-type and E43K/D44K double mutant SilPcs.

MATERIALS AND METHODS

Crystallization—Crystallization of the wild-type SilPc has already been reported (*12*). A mutant SilPc was expressed in *Escherichia coli* and purified by the procedure described by Lee *et al.* (*11*). Screening for the crystallization conditions was carried out in a similar way to that for the wild-type crystallization using ammonium sulfate as a precipitant. Crystallization was performed by the hanging-drop vapor diffusion method (*13*). The drops consisted of 3 μl of a protein solution and 3 μl of a precipitating solution. Plate-like crystals (0.4×0.4×0.6 mm) were obtained at room temperature after 2-3 weeks in 2.8 M ammonium sulfate and 100 mM potassium phosphate (pH 7.0) when the protein solution was concentrated to 13 mg·ml^{-1} in Milli-Q water.

X-Ray Diffraction Study—X-Ray diffraction experiments were carried out using an R-AXIS IIc imaging-plate area detector mounted on an Rigaku RU-300 rotating-anode source with Cu$K\alpha$ radiation. The space group of the wild-type SilPc crystals was determined to be trigonal

[1] This study was partially supported by Grants-in-Aid for Scientific Research on Priority Areas, #07780572 and #09780632, from the Ministry of Education, Science, Sports and Culture of Japan, to T.I.
[2] Present address: Department of Biochemistry, School of Medicine, Case Western Reserve University, 10900 Euclid Ave, Cleveland, Ohio 44106-4935, USA.
[3] To whom correspondence should be addressed. E-mail: kai@ap.chem.eng.osaka-u.ac.jp
Abbreviation: SilPc, plastocyanin from *Silene*.

$P3_121$ or $P3_221$ with unit cell parameters of $a=b=76.6$, and $c=65.5$ Å. Assuming two molecules of wild-type SilPc per asymmetric unit, the Matthews constant (*14*) is $V_m=2.64$ Å^3·Da^{-1}. The space group of the mutant SilPc crystals was determined to be tetragonal $P4_12_12$ or $P4_32_12$ with unit cell parameters of $a=b=55.9$, and $c=68.2$ Å. Assuming one molecule of mutant SilPc per asymmetric unit, the Matthews constant is $V_m=2.54$ Å^3·Da^{-1}. The diffraction data were processed using programs *DENZO* and *SCALEPACK* (*15*). The final data for the wild-type SilPc crystals comprised 11,515 independent reflections and completeness of 94.2% from 44,196 total reflections in the range of 30-2.0 Å with an overall R_{merge} of 6.0%. The final data for the mutant SilPc crystal comprised 10,737 independent reflections and completeness of 93.6% from 52,627 total reflections in the range of 30-1.75 Å with an overall R_{merge} of 5.6%.

Structure Determination—The crystal structures of the wild-type and mutant SilPcs were solved by the molecular replacement method. The search model for wild-type SilPc was based upon poplar plastocyanin (PDB code 1PCY) (*4*). The search model for mutant SilPc was based upon the wild-type SilPc. Molecular replacement calculations were performed using program *AMoRe* (*16*). Supposing that the space group of wild-type SilPc belonged to $P3_221$, two outstanding peaks appeared with an R-factor of 30.7% (8-4 Å) on translation function calculations. In the mutant SilPc, supposing that the space group belonged to $P4_32_12$, a clear solution was found. The model was refined by the use of programs *X-PLOR* (*17*) and *REFMAC* (*18*). After the application of one round of the simulated annealing protocol, multiple cycles of alternate model fitting and refinements were performed. The quality of the final model was assessed by means of Ramachandran plots and analysis of the model geometry with program *PROCHECK* (*19*). The plots for the wild-type and mutant SilPcs indicated that 90.6 and 91.2% of the residues lay in the most favored regions, and 9.4 and 8.8% in additional allowed regions, respectively. The final R and R_{free} factors for all reflections between 20.0 and 2.0 Å resolution for the wild-type SilPc were 0.189 and 0.225, respectively. The final R and R_{free} factors between 20.0 and 1.75 Å resolution for the mutant SilPc were 0.180 and 0.199, respectively. The refinement statistics are summarized in Table I. The coordinates for the wild-type and mutant SilPcs have been submitted to the Protein Data Bank under accession numbers 1BYO and 1BYP, respectively.

TABLE I. **Refinement statistics.**

	Wild-type	Mutant
Resolution (Å)	20-2.0	20-1.75
No. of protein molecules	2	1
No. of protein atoms	1464	733
No. of water molecules	78	73
No. of reflections		
Working set	10,929	10,216
Test set for R_{free}	568	515
R (%)	18.9	18.0
R_{work} (%)	19.7	18.8
R_{free} (%)	22.5	19.9
Root mean square deviation from standard geometry		
Bond length (Å)	0.016	0.013
Bond angle (degrees)	2.46	2.46
Ramachandran plot		
Residues in most favored regions (%)	90.6	91.2
Residues in additional allowed regions (%)	9.4	8.8

RESULTS AND DISCUSSION

Quality of the Final Model—The final model for the wild-type SilPc is made up of two monomers per asymmetric unit inclusive of 78 water molecules. The root mean square deviations from the ideal geometry of the bond lengths and angles are 0.016 Å and 2.46°, respectively. The final model for the mutant SilPc is made up of one monomer per asymmetric unit including 73 water molecules. The root mean square deviations from the ideal geometry of the bond lengths and angles are 0.013 Å and 2.46°, respectively. Both the wild-type and mutant SilPcs remained close to the standard geometry throughout the refinement. Well defined electron density maps were obtained for all residues in both the wild-type and mutant SilPcs. The mean coordinate errors for the atoms estimated from Luzzati plots are 0.217 and 0.164 Å for the wild-type and mutant SilPcs, respectively (*20*). The quality of the final model is summarized in Table I.

Overall Structures—The wild-type SilPc comprises two monomers per asymmetric unit (SilPc A and B). A ribbon drawing of SilPc A is presented in Fig. 1. The two plastocyanin monomers show root mean square deviations for all protein atoms of 0.82 Å. Both SilPcs consist of two β-sheets in common with other plastocyanins. The secondary structures of the SilPcs were determined with program *DSSP* (*21*). SilPc A has eight β-strands and one α-helix, however, SilPc B has no α-helix. The secondary

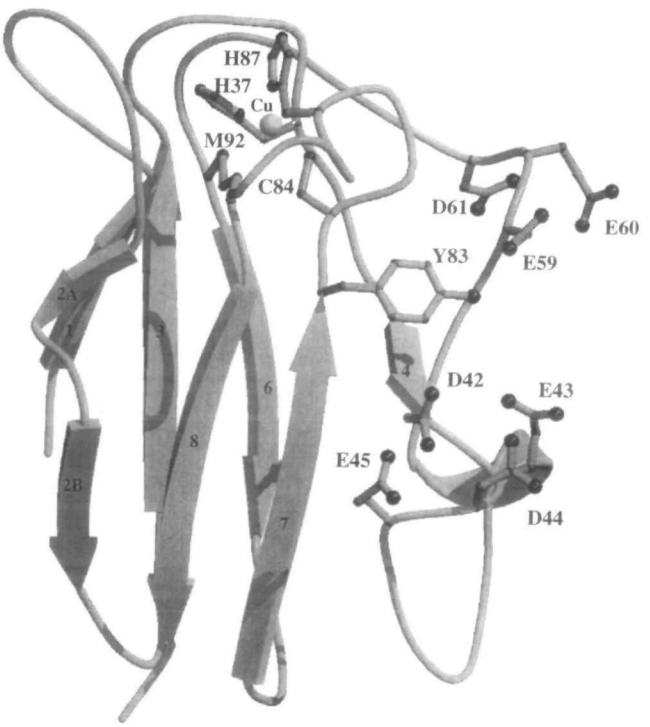

Fig. 1. **Schematic representation of the structure of SilPc A.** The numbers are those of the β-strands. This figure was drawn by means of program *MOLSCRIPT* (*23*) and rendered by means of program *RASTER3D* (*24*).

structures of SilPc A are identical with those of poplar and spinach plastocyanins. The mutant SilPc as well as SilPc A have eight β-strands and one α-helix. The mutant SilPc as well as poplar and spinach plastocyanins have a 3_{10} helix at residues 85-87. Compared with SilPc A and B, there are significant structural differences in the main chain of residues 8-10 and the side chains of residues 42-45. The root mean square deviation for the side chain atoms of residues 42-45 between SilPc A and B is 1.60 Å. The carboxylate oxygen atoms of these side chains have relatively high temperature factors of more than 45 and 41 Å^2, respectively. These side chains indicate that the side chains of residues 42-45 have flexibility. The flexibility of residues 42-45 is significant because the side chains of these residues are essential for electron transfer (*11*). In the structure of the complex of spinach plastocyanin and turnip cytochrome *f* determined by means of NMR and molecular dynamics, the side chains of D42, E43, and D44 in plastocyanin are close to those of R209, K187, and K185 in cytochrome *f*, respectively (*22*). The flexibility of these side chains seems to be effective for the formation of ion pairs between plastocyanin and cytochrome *f*.

Copper Geometry—In plastocyanins, the copper site exhibits a distorted tetrahedral geometry. The copper geometries of SilPc A and the mutant SilPc show little difference with those of other plastocyanins. The distance between the copper ion and the $N_{\delta 1}$ atom of H87 in SilPc B is a little greater (2.31 Å) than those in SilPc A and other plastocyanins (Fig. 2A). The side chain of H87 in SilPc B forms a hydrogen bond bridge to the main chain carbonyl oxygen of G10 from neighboring SilPc B through a water molecule (Fig. 2B). That of H87 in SilPc A also forms a hydrogen bond with a water molecule, however, there is no hydrogen bond bridge to G10. The side chain of H87 in SilPc B undergoes a van der Waals interaction with that of symmetry-related L12 (3.5 Å apart) (Fig. 2B). These interactions cause the unusually great distance between the copper ion and the $N_{\delta 1}$ atom of H87 in SilPc B.

Comparison with Other Higher Plant Plastocyanins—The sequence identity between SilPc and poplar or spinach plastocyanin is 71 and 79%, respectively. The root mean square deviation between SilPc A and poplar or spinach plastocyanin is 0.52 or 0.57 Å for the Cα atoms, respectively. The structure of SilPc is similar to those of poplar and spinach plastocyanin. On Comparison of the wild-type SilPc, and poplar and spinach plastocyanins, significant

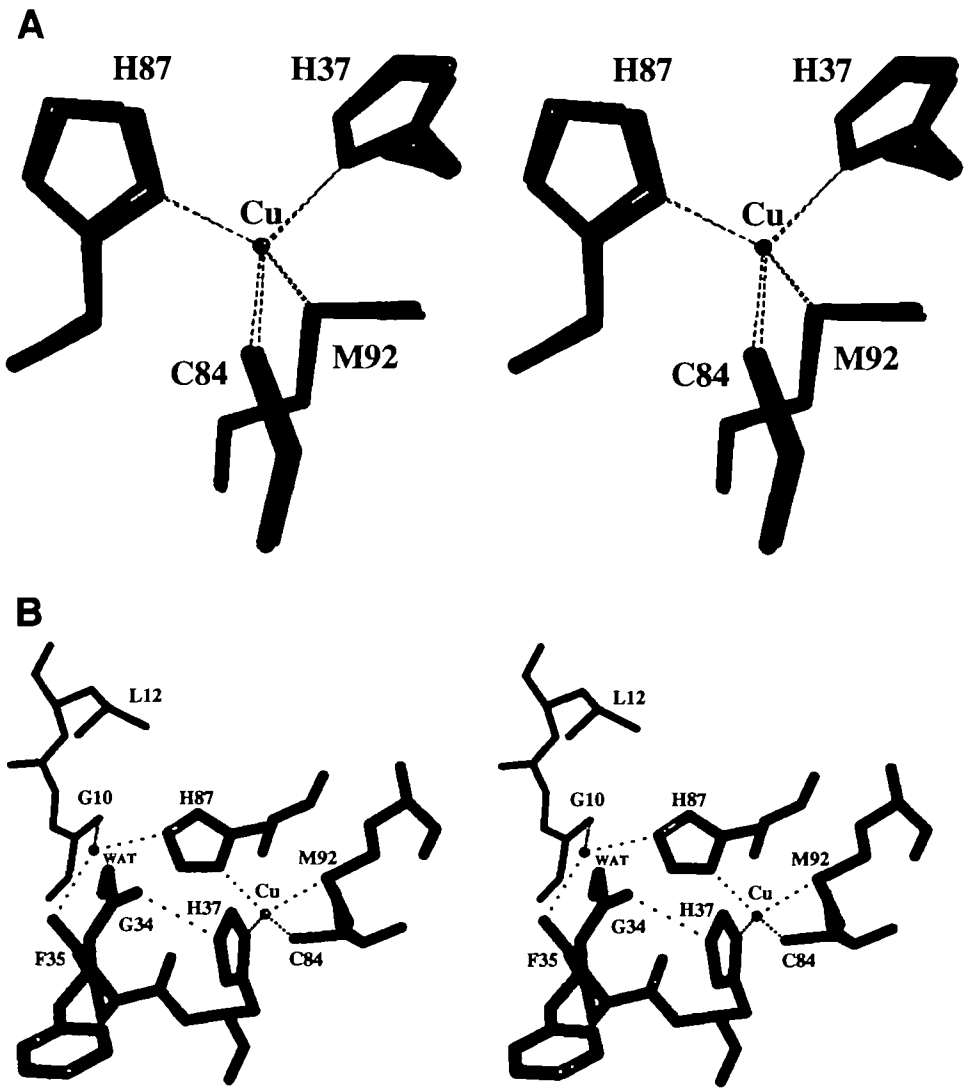

Fig. 2. **A: Stereo-view of the copper binding site of SilPc A (thick and light lines) compared with that of SilPc B (thin and dark lines). B: Stereo-view of the structures around H87 of SilPc B (thick and light lines) and the symmetry-related positions 10 to 12 (thin and dark lines).** These figures were drawn by means of program *MidasPlus* (*25, 26*).

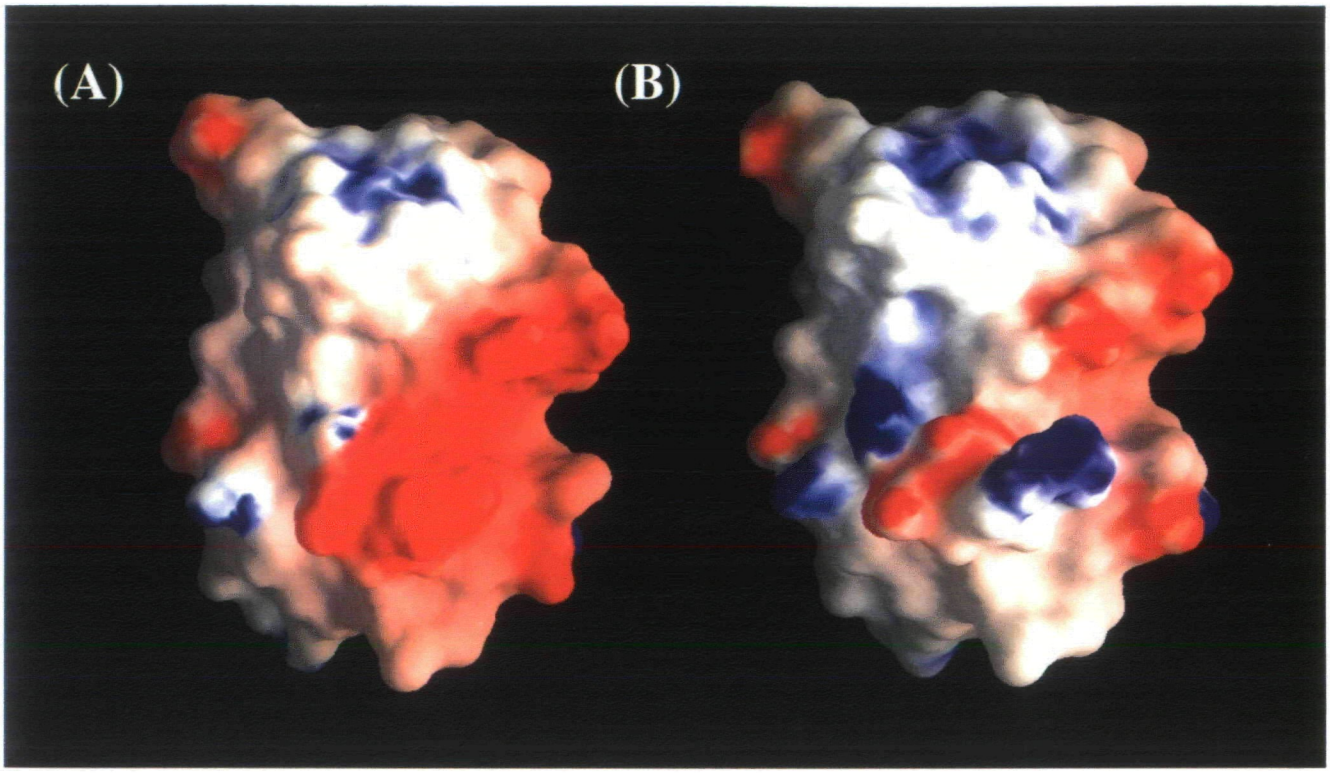

Fig. 3. **Electrostatic surface potentials of SilPc A (A) and the mutant SilPc (B) as viewed in relatively the same orientation.** Red areas correspond to negatively and blue ones to positively charged potentials. These figures were drawn by means of program *GRASP* (*27*).

structural differences were found in the main chain of G67. In poplar and spinach plastocyanins, the amide nitrogen of G67 forms a hydrogen bond with the carbonyl oxygen of N31. In the wild-type SilPc, there is no corresponding hydrogen bond, however, the ε-amino group of K30 forms an ion pair with the carboxylate group of E2. On comparison of the wild-type SilPc and spinach plastocyanins, significant structural differences were also found in the main chains of E59 and E60. In spinach plastocyanin, crystal packing interactions were observed around these residues, which resulted in the structural differences (*5*).

Comparison of the Wild-Type and Mutant—The root mean square deviation for Cα atoms between mutant SilPc and SilPc A is 0.44 Å. On comparison of the wild-type and mutant SilPcs, significant structural differences were found in the main chain of G67. In the mutant SilPc as well as the wild-type one, the amide nitrogen of G67 forms no hydrogen bond with the carbonyl oxygen of N31. In the mutant SilPc, the ε-amino group of K30 forms an ion pair with the carboxylate group of E69 instead of that of E2 in the wild-type one. The root mean square deviation for backbone atoms of residues 42-45 between SilPc A and the mutant SilPc is 0.18 Å. The main chain structure of the mutant SilPc around residues 43 and 44 is very similar to that of the wild-type SilPc. Therefore, there is little structural change due to mutation of residues 43 and 44 between the wild-type and mutant SilPcs.

Features of the Molecular Surface and Its Relationship with the Acidic Patch—An electrostatic potential map of the molecular surface shows a large negatively charged region in the wild-type SilPc (Fig. 3A). In the mutant SilPc, the negatively charged region is divided into very small sites (Fig. 3B), suggesting that residues 43 and 44 of plastocyanin play a primary role in the formation of the negatively charged surface region. The side chains of these two residues in SilPc are exposed and located in the outermost surface region of the molecule. Thus, they seem to play an important role in the molecular recognition of the electron transfer reaction. The decrease in the negatively charged surface region which results from mutations of residues 43 and 44 is linked to those of the electron-transfer rates from cytochrome *f* and to $P700^+$, because little structural differences around the main chains of residues 43 and 44 were found between the wild-type and mutant SilPcs. That is to say, the decrease in the negatively charged surface region must cause those in the electron-transfer rates.

REFERENCES

1. Aitken, A. (1976) Protein evolution in cyanobacteria. *Nature* **263**, 793-796
2. Sandmann, G. (1986) Formation of plastocyanin and cytochrome *c*-553 in different species of blue-green algae. *Arch. Microbiol.* **145**, 76-79
3. Sandmann, G., Reck, H., Kessler, E., and Boger, P. (1983) Distribution of plastocyanin and soluble plastidic cytochrome *c* in various classes of algae. *J. Gen. Microbiol.* **134**, 23-27
4. Guss, J.M., Bartunik, H.D., and Freeman, H.C. (1992) Accuracy and precision in protein structure analysis: restrained least-squares refinement of the structure of poplar plastocyanin at 1.33 Å resolution. *Acta Crystallogr.* **B48**, 790-811
5. Xue, Y., Ökvist, M., Hansson, Ö., and Young, S. (1998) Crystal

structure of spinach plastocyanin at 1.7 Å resolution. *Protein Sci.* **7**, 2099-2105
6. Moore, J.M., Lepre, C.A., Gippert, G.P., Chazin, W.J., Case, D.A., and Wright, P.E. (1991) High-resolution solution structure of reduced French bean plastocyanin and comparison with the crystal structure of poplar plastocyanin. *J. Mol. Biol.* **221**, 533-555
7. Bagby, S., Driscoll, P.C., Harvey, T.S., and Hill, H.A.O. (1994) High-resolution structure of reduced parsley plastocyanin. *Biochemistry* **33**, 6611-6622
8. Gross, E.L. (1996) *Oxygenic Photosynthesis: The Light Reactions* (Ort, D.R. and Yocum, C.F., eds.) pp. 413-429, Kluwer Academic Publishers, Dordrecht
9. Navarro, J.A., Hervás, M., and De la Rosa, M.A. (1997) Co-evolution of cytochrome c_6 and plastocyanin, mobile proteins transferring electrons from cytochrome b_6f to photosystem I. *J. Biol. Inorg. Chem.* **2**, 11-22
10. Kannt, A., Young, S., and Bendell, D.S. (1996) The role of acidic residues of plastocyanin in its interaction with cytochrome *f*. *Biochim. Biophys. Acta* **1277**, 115-126
11. Lee, B.H., Hibino, T., Takabe, T., Weisbeek, P.J., and Takabe, T. (1995) Site-directed mutagenetic study on the role of negative patches on *Silene* plastocyanin in the interactions with cytochrome *f* and photosystem I. *J. Biochem.* **117**, 1209-1217
12. Li, C., Inoue, T., Gotowda, M., Hamada, K., Nishio, N., Hibino, T., Takabe, T., and Kai, Y. (1997) Crystallization and preliminary X-ray studies of plastocyanin from *Silene* expressed in *E. coli*. *Acta Crystallogr.* **D53**, 129-130
13. McPherson, A. (1982) *Preparation and Analysis of Protein Crystals*, 1st ed., pp. 96-97, John Wiley, New York
14. Matthews, B.W. (1968) Solvent content of protein crystals. *J. Mol. Biol.* **33**, 491-497
15. Otwinowski, Z. (1993) Proceedings of CCP4 Study Weekend 1993 (Sawyer, L., Issacs, N., and Bailey, S., eds.) pp. 56-62, Daresbury Laboratory, Warrington
16. Navaza, J. (1994) AmoRe: an automated package for molecular replacement. *Acta Crystallogr.* **A50**, 157-163
17. Brünger, A.T., Kuriyan, J., and Karplus, M. (1987) Crystallographic *R*-factor refinement by molecular dynamics. *Science* **235**, 458-460
18. Murshudov, G.N., Vagin, A.A., and Dodson, E.J. (1997) Refinement of macromolecular structures by the maximum-likelihood method. *Acta Crystallogr.* **D53**, 240-255
19. Laskowski, R.A., MacArthur, M.W., Moss, D.S., and Thornton, J.M. (1993) PROCHECK: a program to produce both detailed and schematic plots of protein structures. *J. Appl. Crystallogr.* **26**, 283-291
20. Luzzati, V. (1952) Traitement statistyique des erreurs dans la détermination des structures cristallines. *Acta Crystallogr.* **5**, 802-810
21. Kabsch, W. and Sander, C. (1983) Dictionary of protein secondary structure: Pattern recognition of hydrogen-bonded and geometrical features. *Biopolymers* **22**, 2577-2637
22. Ubbink, M., Ejdebäck, M., Karlsson, B.G., and Bendell, D.S. (1998) The structure of the complex of plastocyanin and cytochrome *f*, determined by paramagnetic NMR and restrained rigid-body molecular dynamics. *Structure* **6**, 323-335
23. Kraulis, P.J. (1991) MOLSCRIPT: a program to produce both detailed and schematic plots of protein structures. *J. Appl. Crystallogr.* **24**, 946-950
24. Merritt, E.A. and Murphy, M.E.P. (1994) Raster3D version 2.0 —a program for photorealistic molecular graphics. *Acta Crystallogr.* **D50**, 869-873
25. Ferrin, T.E., Huang, C.C., Jarvis, L.E., and Langridge, R. (1988) The MIDAS display system. *J. Mol. Graphics* **6**, 13-27
26. Huang, C.C., Pettersen, E.F., Klein, T.E., Ferrin, T.E., and Langridge, R. (1991) Conic: A fast renderer for space-filling molecules with shadows. *J. Mol. Graphics* **9**, 230-236
27. Nicholls, A., Sharp, K.A., and Honig, B. (1991) Protein folding and association: insights from the interfacial and thermodynamic properties of hydrocarbons. *Proteins* **11**, 281-296